Japanese Journal of Applied Physics
Vol. 44, No. 10, 2005, pp. 7662–7666

Novel Method for *In Situ* Monitoring of Thickness of Quartz during Wet Etching

Chi-Yuan LEE*, Pei-Zen CHANG[1], Yung-Yu CHEN[1], Ching-Liang DAI[2], Ping-Hei CHEN[3] and Shuo-Jen LEE

Department of Mechanical Engineering, Yuan Ze University, Taoyuan, Taiwan, R.O.C.
[1]*Institute of Applied Mechanics, National Taiwan University, Taipei, Taiwan, R.O.C.*
[2]*Department of Mechanical Engineering, National Chung Hsing University, Taichung, Taiwan, R.O.C.*
[3]*Department of Mechanical Engineering, National Taiwan University, Taipei, Taiwan, R.O.C.*

(Received June 2, 2005; accepted June 25, 2005; published October 11, 2005)

In this work, we present a novel method based on a plate wave sensor for the *in situ* monitoring of the thickness of quartz membranes during wet etching. Similarly to oscillators and resonators, some acoustic devices require the thickness of quartz membranes to be determined precisely. Precise control of the thickness of quartz membranes during wet etching is important, because the thickness strongly influences post processing and frequency control. Furthermore, the proposed plate wave sensor, allows the thickness of quartz membranes from a few μm to hundreds of μm to be monitored *in situ*, which depends on the periodicity of an interdigital transducer (IDT). In summary, the proposed method for measuring the thickness of quartz membranes in real time has a high accuracy, is simple to set up and can be mass-produced. Also described herein are the principles of the method used, the detailed process flow, the measurement set up and the simulation and experimental results. The theoretical and measured values differ by an error of less than 1 μm, implying a close correspondence.
[DOI: 10.1143/JJAP.44.7662]

KEYWORDS: plate wave sensor, *in situ* monitoring, IDT

1. Introduction

Surface acoustic wave (SAW) devices are primarily used as high-performance signal processing devices, such as filters and delay lines.[1,2] Additionally, electronic devices that use acoustic propagation have been successfully used as filters and resonators in cellular phones, television sets and other communication systems. New developments in mobile communication systems require higher operating frequencies, smaller sizes and lighter equipment. Therefore, various oscillators and resonators must be miniature models with a high operating frequency. A higher operating frequency is obtained using a thinner substrate (quartz), because the frequency of the resonator is inversely proportional to the thickness of the membrane. Quartz has been thinned by various techniques including wet etching,[3] plasma etching[4,5] and mechanical polishing.[6] Wet etching using a buffered HF solution is a method well-adapted for mass production while plasma etching provides high precision in controlling frequency.[7] The advantages and disadvantages of wet and dry etchings are well known.[8] With mechanical restrictions on fabricating resonators, 50 MHz has been the upper limit of the fundamental operating frequency at a quartz thickness of about 33 μm.[9] Even if a thinner substrate could be lapped and polished, implementing mass production and ensuring high reliability would be difficult.

Wet etching was the key technology for fabricating various SAW devices (oscillators and resonators) on a quartz substrate. A high-frequency fundamental (HFF) quartz resonator with a frequency range from 80 MHz to nearly 1 GHz in the fundamental mode, is fabricated by industrial photolithographic batch manufacturing using wet etching.[9] Thus, the *in situ* precise monitoring of the thickness of a quartz membrane during wet etching is important, because the thickness strongly influences post-processing and frequency control. The crystal etch monitoring (CEM) instrument measures the resonance frequency of piezoelectric resonators during etching using special electrodes close to the blank in conductive fluids.[10,11] However, this method can be applied only in conductive fluids to measure the thickness of a quartz membrane. Also this method is difficult for monitoring the thickness of a crystal blank wafer. In this work, another principle is proposed and a method is developed for use even in a non conductive fluid and for monitoring the thickness of a whole quartz wafer.

2. Methodology

2.1 *Plate waves that propagate in piezoelectric plate loaded with viscous liquid*

In this paper, eight-dimensional matrix formalism was applied to study plate wave propagation in piezoelectric plates loaded with a viscous liquid.[12] The dispersion equation of plate waves in such a structure is formulated under continuity conditions at the solid–liquid interface. With this formulation, the size of the matrix encountered in the computation is independent of the number of layers.

Consider a piezoelectric plate loaded with a viscous liquid in a half-space, where the interface is at $z = H$, as shown in Fig. 1. According to eight-dimensional matrix formalism, at the interface, the relationship between the generalized traction vector $\boldsymbol{T}$ and the generalized velocity vector $\boldsymbol{V}$ is expressed as

$$\boldsymbol{T}(H^-) = \boldsymbol{G}\boldsymbol{V}(H^-) \tag{1}$$

where $\boldsymbol{G}$ is the 4×4 impedance tensor, and H is the plate thickness. In a viscous liquid half-space, because only up going waves exist, the global impedance is equivalent to the up going wave impedance $\boldsymbol{Z}_1$. Therefore, the corresponding relation at the boundary of the viscous liquid is given by

$$\boldsymbol{T}_1(H^+) = \boldsymbol{Z}_1\boldsymbol{V}_1(H^+) \tag{2}$$

At the liquid–solid interface, the stress, particle velocity, electric potential and electric displacement must satisfy the continuity condition

$$\boldsymbol{T}(H^-) = \boldsymbol{T}_1(H^+), \quad \boldsymbol{V}(H^-) = \boldsymbol{V}_1(H^+) = \boldsymbol{V}(H). \tag{3}$$

*Correspondence author. E-mail address: cylee@saturn.yzu.edu.tw

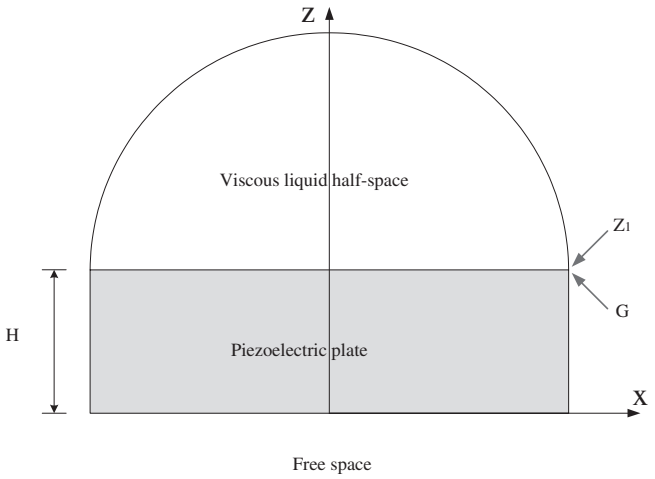

Fig. 1. Configuration of piezoelectric plate loaded with viscous liquid in half-space.

From eqs. (1)–(3), we obtain

$$(\boldsymbol{G} - \boldsymbol{Z}_1)\boldsymbol{V}(H) = 0. \tag{4}$$

The non trivial solution of the generalized velocity vector $\boldsymbol{V}(H)$ exists only if

$$\det(\boldsymbol{G} - \boldsymbol{Z}_1) = 0 \tag{5}$$

Equation (5) is also called the dispersion equation for the propagation of plate waves in a piezoelectric plate loaded with the viscous liquid in a half-space. The generalized velocity vector at the liquid–solid interface can be obtained by substituting the wave number k_x in the x-direction and the circular frequency ω, both of which satisfy eq. (5). The generalized traction vector at the interface can be determined by substituting the generalized velocity vector into eq. (4). Once the two generalized vectors are known, the stress, particle velocity, electric potential and electric displacement at any positions in the liquid or solid part can be evaluated.

Here, the formulation based on the surface impedance tensor method was utilized to calculate the dispersion curve of a viscous-liquid-loaded AT-cut quartz substrate. The relevant constants utilized in the calculations are cited from ref. 13. Table I lists the material constants used in this calculation. Figures 2(a) and 2(b) present the simulation results, which are the phase velocities with respect to the product of the wave number and quartz thickness. According to the simulation results, the phase velocity approaches the velocity of the Rayleigh wave of quartz when the product of the wave number and quartz thickness increases in liquid. When the quartz is thinner, the wavelength of the acoustic, surface acoustic and bulk waves combine into a plate wave, and the phase velocity changes with the thickness of the quartz substrate. Therefore, the simulation accuracy of the phase velocity of this plate wave is very important.

Table I. Material constants used in simulation.

		Quartz	Water
Elastic constant (10^{10} N/m^2)	C_{11}	8.674	
	C_{12}	0.699	
	C_{13}	1.191	
	C_{14}	−1.791	
	C_{33}	10.72	
	C_{44}	5.794	
Piezoelectric constant (C/m^2)	e_{11}	0.171	
	e_{14}	−0.0436	
Relative dielectric constant	ε_{11}	4.5	80.359
	ε_{33}	4.6	
Mass density (10^3 kg/m^3)	ρ	2.651	0.997
Longitudinal wave velocity (m/s)	C_L		1500
Viscosity (10^{-4} N s/m^2)	μ_L		8.9

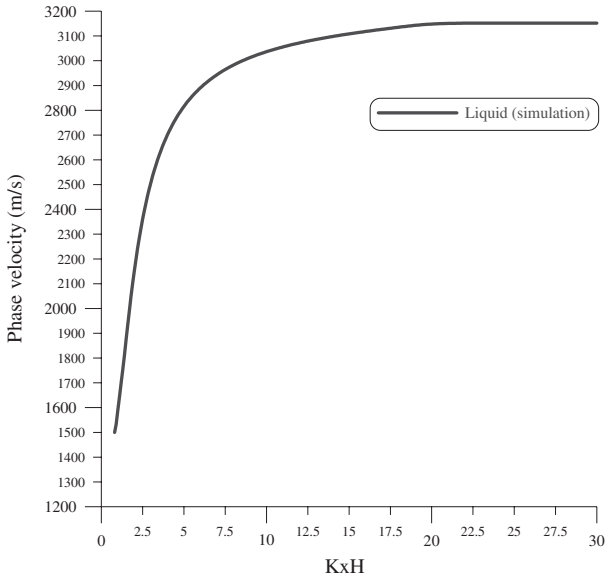

(a)

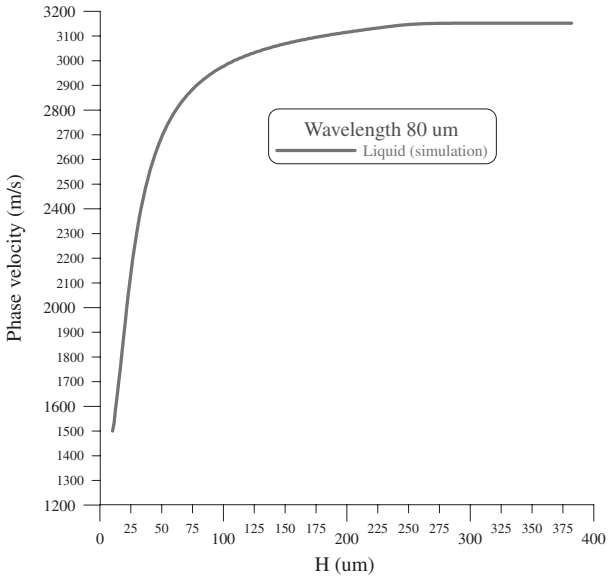

(b)

Fig. 2. Dispersion curve of viscous-liquid-loaded AT-cut quartz substrate: (a) product of wave number and quartz thickness vs phase velocity and (b) thickness of quartz vs phase velocity.

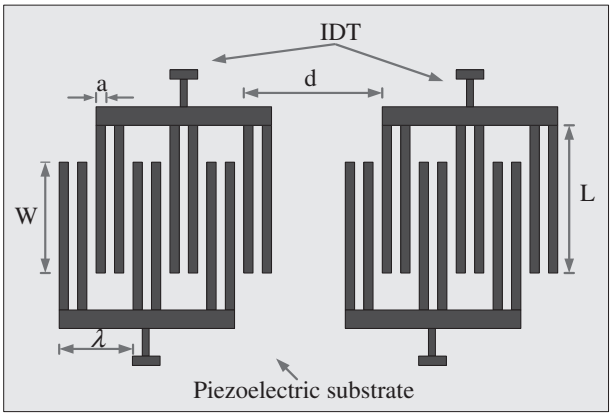

Fig. 3. Schematic of configuration of IDT.

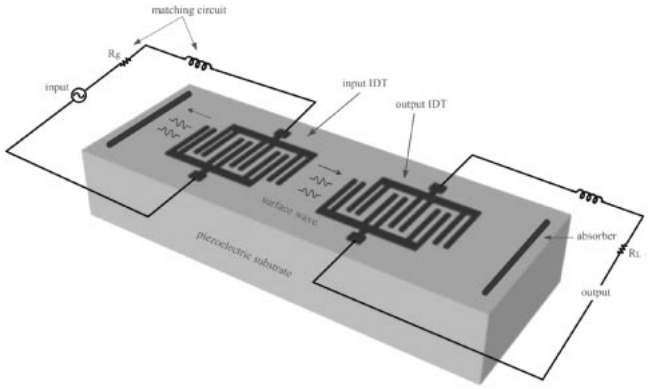

Fig. 4. Schematic diagram of plate wave sensor.

2.2 *Design of plate wave sensor*

An associated electrostatic wave exists for a plate wave on a piezoelectric substrate, which allows electroacoustic coupling via a transducer.[14] Quartz has been the material of choice since its high Q (quality factor) and high stiffness makes it the primary frequency and frequency-stability determining element in a crystal oscillator. A plate wave sensor was fabricated on an AT-cut quartz substrate using two ports of a split-electrode interdigital transducer (IDT). The piezoelectric effect was such that, when the AC voltage was applied to the split electrode of the input IDT, and signal voltage variations were subsequently converted into a mechanical acoustic wave, the other IDT was used as an output receiver to convert mechanical wave vibrations back into output voltage.[15] Output voltage or wave velocity changed with the thickness of the quartz substrate.

Figure 3 shows the configuration of IDT, where λ is the periodicity of IDT (wavelength of the acoustic wave), L is the length of IDT fingers, W is the length of the overlap of IDT fingers (acoustic aperture), and d is the length of the path of acoustic propagation. In the design of IDT, a number of parameters have to be specified. The spacing and electrode width will determine the frequency response of the transducer. In the proposed design, a split-electrode IDT was selected, because the problem that results from finger reflections can be greatly diminished using a $\lambda/8$ finger width instead of a $\lambda/4$ finger width, such that SAW reflections from each split-electrode pair cancel out at the center frequency, rather than adding as in the case of a single-electrode IDT.[15] Table II list the parameters of the IDT design used in our experiment.

Table II. IDT design parameters.

Interdigital transducer (IDT)	Value of parameter
Periodicity of IDT, λ (μm)	80
Length of IDT fingers, L (μm)	3600
Length of overlap of IDT fingers, W (μm)	2800
Length of path of acoustic propagation, d (μm)	1200
Number of pairs, N	80
Area of pad (μm^2)	80×80

3. Fabrication

This plate wave sensor was fabricated by the process illustrated in Fig. 4. The process was started with an AT-cut 392-μm-thick 76-mm-diameter quartz. First, on the rear side of the quartz substrate, Shipley S1813 photoresist was coated using a spinner that rotated at a rate of 1000 rpm for 5 s, and then at 4000 rpm for 40 s. The coated substrate was then soft-baked at 90°C for 100 s, and the etching-hole area pattern was exposed onto the photoresist-coated substrate surface using ultraviolet light, as shown in Fig. 5(a). To enhance the adhesion of Au film, a Cr film of about 100 Å thick was evaporated before Au film with a thickness of 900 Å was evaporated: both processes involved a thermal evaporator, as shown in Fig. 5(b). Unwanted Cr and Au films were lifted off by soaking the substrate in acetone to form a rear-side etching hole, as shown in Fig. 5(c). Care was taken to ensure the success of the lift-off process. Several causes of the failure of lift-off may apply, such as the lack of an undercut photoresist pattern, the non vertical evaporation of Au, poor Au film adhesion and substrate surface contamination.[16] A Au film was used as an etching mask during wet etching in NH_4HF_2 solution. IDTs were patterned using semiconductor photolithographic techniques, which involved the deposition of Al with a thickness of 900 Å by electron beam evaporation, as shown in Fig. 5(d). Finally, a quartz membrane was formed by soaking the rear of the substrate at 65°C in 50 wt % NH_4HF_2 solution, and the etching rate was approximately 2.85 μm/h, as shown in Fig. 5(e).

4. Results

The experimental setup for measuring the frequency response and insertion loss of a plate wave sensor, as illustrated in Fig. 6, includes an HP8714ES network analyzer and an etching holder. An HP8714ES network analyzer monitor with a frequency resolution of 0.01 MHz was used to monitor in real time the thickness of the quartz membrane as the target central frequency was shifted. When the central frequency shifts, the thickness of the quartz membrane can be determined based on the amount of shift in the central frequency. The measurement accuracy of the central frequency was 0.01 MHz; the thickness of quartz membrane accuracy was 0.05 μm. The etching process automatically monitors the thickness of the quartz membrane as the frequency shifts. First, an alpha-step 500 surface profiler was used to measure the initial total thickness of 396.10-μm-

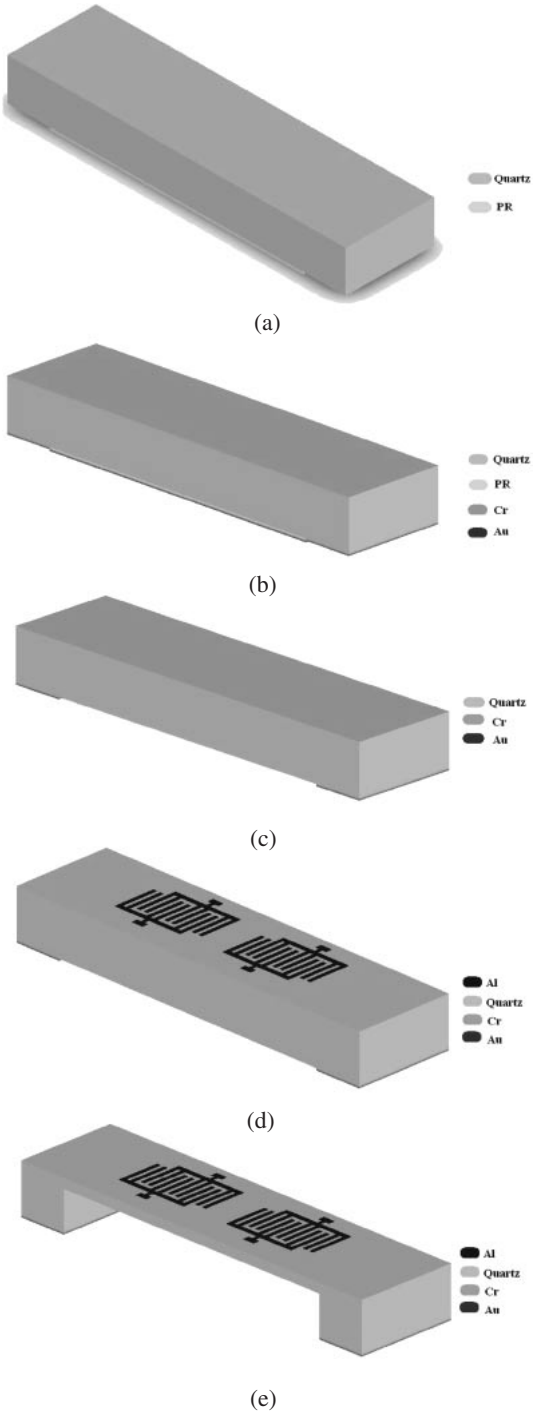

Fig. 5. Process flow of plate wave sensor: (a) Coating photoresist to define pattern at the rear of etching hole, (b) Evaporating Cr/Au film, (c) Forming pattern on rear side of etching hole, (d) Evaporating Al film and pattern-defining IDTs, and (e) NH_4HF_2-etch-forming quartz membrane.

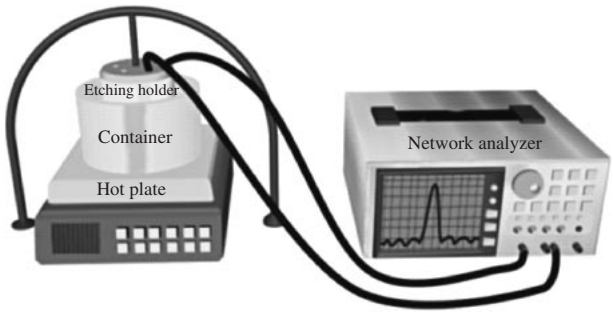

Fig. 6. Experimental setup of plate wave sensor.

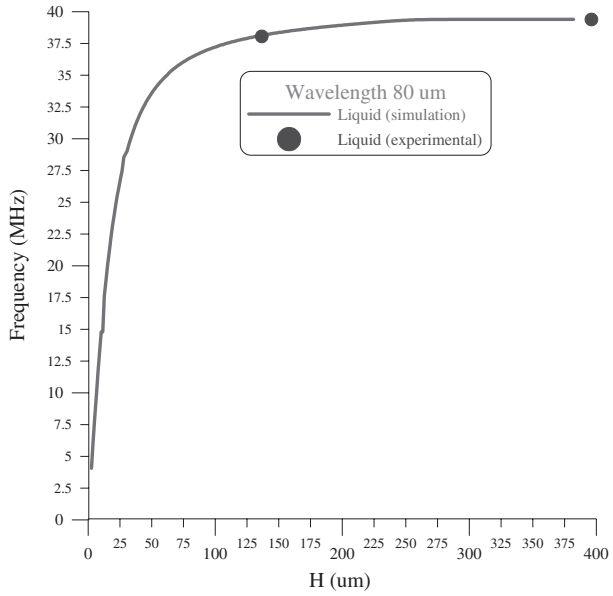

Fig. 7. Comparison of simulation and experimental results of thickness of quartz with respect to frequency.

thick quartz. The central frequency of the experimental unetched wafer was 39.39 MHz. Then, the etched of quartz was measured at 136.60 μm thick. An experimental result of the etched central frequency was 38.06 MHz, the experimental results described in Table III. A quartz membrane was formed by soaking the rear of the substrate at 65°C in 50 wt % in NH_4HF_2 solution, and the etching rate was approximately 2.85 μm/h. Therefore, etching the quartz substrate took more than 91 h. The NH_4HF_2 solution penetrated the epoxy, thus destroying the sensor. Figure 7 shows a comparison of the simulation and experimental results of quartz thickness with respect to frequency. Figure 7 reveals that the error between the simulation and experimental results is within 1 μm, implying a close correspondence.

Table III. Experimental results.

	Etch depth of quartz (μm)	Thickness of quartz (μm)	Central frequency (MHz)	Amount of shift in central frequency (MHz)	Insertion loss S_{21} (dB)
Unetched quartz	0	396.10	39.39	0	−22.57
Etched quartz	259.50	136.60	38.06	1.33	−46.53

5. Conclusions

In this work, we present a plate wave sensor for monitoring the thickness of a quartz membrane in real time during wet etching. Also described herein are the principles of the method used, the detailed process flow, the measurement set up, and the simulation and experimental results. The error between the theoretical and measured values is within 1 μm, implying a close correspondence.

Acknowledgements

This work was accomplished with much needed support and the authors would like to thank the financial support received from the National Science Council of R.O.C. through the grant NSC 94-2212-E-155-006. The authors also like to thank Chi-Lieh Hsieh, and Chih-Wei Chuan of the Department of Mechanical Engineering, Yuan Ze University, Shih-Yung Pao, Kai-Hsiang Yen, Fu-Yuan Xiao, Ying-Chou Cheng, Wen-Jong Chen, Chih-Wei Liu, Chia-Hua Chu and Xuan-Yu Wang of the Institute of Applied Mechanics, National Taiwan University, Professors Tsung-Tsong Wu, Lung-Jieh Yang and Chien-Liu Chang for their valuable advice and assistance in experiment. In addition, we would, finally, like to thank the NTU Nano-Electro-Mechanical-Systems Research Center for providing access to their research facilities.

1) D. P. Morgan: *Surface Wave Devices for Signal Processing* (Elsevier, Amsterdam, 1985).
2) C. K. Campbell: *Surface Wave Devices and Their Signal Processing Applications* (Academic Press, Boston, 1989).
3) O. Ishii, T. Morita, T. Saito and Y. Nakazawa: IEEE Int. Frequency Control Symp., 1995, p. 818.
4) K. M. Lakin, G. R. Kline and K. T. McCarron: IEEE Int. Frequency Control Symp., 1995, p. 827.
5) Y. Nagaura and S. Yokomizo: IEEE Int. Frequency Control Symp., 1999, p. 425.
6) Y. Nagaura, K. Kinoshita and S. Yokomizo: IEEE/EIA IEEE Int. Frequency Control Symp. & Exhib., 2000, p. 255.
7) C. Wuthrich, S. D. Piazza, U. Ruedi and B. Studer: IEEE Int. Frequency Control Symp., 1999, p. 807.
8) K. R. Williams and R. S. Muller: J. Microelectromech. Syst. **5** (1996) 256.
9) O. Ishii, H. Iwata, M. Sugano and T. Ohshima: IEEE Int. Frequency Control Symp., 1998, p. 975.
10) F. L. Sauerland: IEEE Int. Frequency Control Symp., 1990, p. 246.
11) F. L. Sauerland: JP Patent H11-234073A (1999).
12) T. T. Wu and M. P. Chang: Jpn. J. Appl. Phys. **41** (2002) 5451.
13) B. A. Auld: *Acoustic Fields and Waves in Solid* (R. E. Krieger, New York, 1990) Vol. I.
14) K. Uchino: *Ferroelectric Devices* (Marcel Dekker, New York, 2000).
15) C. K. Campbell: *Surface Acoustic Wave Devices for Mobile and Wireless Communication* (Academic Press, New York, 1998).
16) S. M. Sze: *VLSI Technology* (McGraw-Hill, New York, 1988).